Published in final edited form as:
Free Radic Biol Med. 2013 December ; 65: . doi:10.1016/j.freeradbiomed.2013.08.191.

The anticancer agent doxorubicin disrupts mitochondrial energy metabolism and redox balance in skeletal muscle

Laura A. A. Gilliam[*,¥], **Kelsey H. Fisher-Wellman**[*,^], **Chien-Te Lin**[*,¥], **Jill M. Maples**[*,^], **Brook L. Cathey**[*,¥], and **P. Darrell Neufer**[*,^,¥]

[*]East Carolina Diabetes and Obesity Institute, East Carolina University, Greenville, NC, USA

[¥]Department of Physiology, East Carolina University, Greenville, NC, USA

[^]Department of Kinesiology, East Carolina University, Greenville, NC, USA

Abstract

The combined loss of muscle strength and constant fatigue are disabling symptoms for cancer patients undergoing chemotherapy. Doxorubicin, a standard chemotherapy drug used in the clinic, causes skeletal muscle dysfunction and premature fatigue along with an increase in reactive oxygen species (ROS). As mitochondria represent a primary source of oxidant generation in muscle, we hypothesized doxorubicin could negatively effect mitochondria by inhibiting respiratory capacity, leading to an increase in H_2O_2 emitting potential. Here we demonstrate a biphasic response of skeletal muscle mitochondria to a single doxorubicin injection (20 mg/kg). Initially at 2 h doxorubicin inhibits both complex I- and II-supported respiration and increases H_2O_2 emission, both of which are partially restored after 24 h. The relationship between oxygen consumption and membrane potential ($\Delta\psi$) is shifted to the right at 24 h, indicating elevated reducing pressure within the electron transport system (ETS). Respiratory capacity is further decreased at a later timepoint (72 h) along with H_2O_2 emitting potential and an increased sensitivity to mitochondrial permeability transition pore (mPTP) opening. These novel findings suggest a role for skeletal muscle mitochondria as a potential underlying cause of doxorubicin-induced muscle dysfunction.

Keywords

chemotherapy; mitochondria; skeletal muscle; reactive oxygen species, ROS; metabolism

INTRODUCTION

Doxorubicin is a potent anthracycline antibiotic used to treat numerous human malignancies [1]. A severe side effect of doxorubicin is cardiotoxicity characterized by a dose-dependent decline in cardiac function with prolonged exposure [2]. Clinicians manage this side effect by limiting the dosage patients receive; however even on a limited dose patients can experience disabling muscle weakness and fatigue [3, 4]. In the clinic, fatigue is generally

Corresponding author: Laura A. A. Gilliam, PhD, Department of Physiology, East Carolina University, 500 Moye Boulevard, Greenville, NC 27858, Phone: (252) 744-2760, Fax: (252) 744-3460, gilliaml@ecu.edu.

documented as perceived fatigue, or a sense of tiredness, which is difficult to distinguish from physiological fatigue [5]. Physiological fatigue involves muscle specific peripheral fatigue, which includes two components: muscle fatigue and muscle weakness. Our previous work suggests the decline in muscle function observed in patients could be due to an effect specifically on skeletal muscle. Healthy rodents exposed to a clinical dose of doxorubicin exhibit a decrease in both hindlimb and respiratory muscle strength, along with an accelerated rate of fatigue [6-8]. The loss of strength in combination with constant fatigue can burden patients, not only during therapy, but up to ten years following the cessation of therapy [9].

Potential mediators of doxorubicin-induced muscle weakness and fatigue are reactive oxygen species (ROS). In cardiac muscle, doxorubicin is known to increase ROS by localizing to the mitochondria [10] where it is reduced by complex I to form a semiquinone radical [11]. In addition, indirect ROS production can occur with doxorubicin through inhibition of the mitochondrial electron transport system (ETS). Previous reports demonstrate doxorubicin inhibits the ETS in isolated heart mitochondria, specifically complexes I and II [12, 13]. An overproduction of oxidants due to a block in the ETS can lead to redox modifications of cell macromolecules (e.g. proteins, lipids, DNA, etc.) with detrimental downstream effects on whole organ function [14, 15].

In skeletal muscle, cytosolic oxidant activity and markers of protein oxidation are elevated following doxorubicin exposure [7, 16]. Mitochondria represent a primary source of oxidant generation in skeletal muscle [17, 18]. Doxorubicin-induced oxidants are blunted in C2C12 myotubes following incubation with Bendavia™ (Stealth Peptides, Newton, MA; formerly known as SS31) [19], a cell-permeable peptide that localizes to the mitochondria and lessens ROS production. These findings suggest doxorubicin could be affecting skeletal muscle mitochondrial function, leading to ROS production.

The objective of this study was to determine the exact nature and extent to which mitochondrial function is impacted by doxorubicin treatment, specifically in skeletal muscle. It was hypothesized doxorubicin would inhibit skeletal muscle mitochondrial respiration, leading to an increase in ROS emitting potential. To test this hypothesis mitochondrial function was evaluated in permeabilized fiber bundles (PmFBs) 2, 24, and 72 h following a single doxorubicin injection (20 mg/kg). The results indicated a biphasic response. Doxorubicin initially (2 h) induced an increase in H_2O_2 emission and membrane potential with a decline in respiratory function that was reversed after 24 h. After 72 h, respiratory capacity was again decreased along with H_2O_2 emitting potential and membrane potential, indicative of a decline in overall mitochondrial function.

METHODS

Overview of experimental design

Male Sprague-Dawley rats (Charles River Laboratories) 8-10 weeks old (~250 g) received an intraperitoneal injection of doxorubicin (20 mg/kg in phosphate buffered saline), a clinically applicable dose that is equivalent to what patients with hematological malignancies receive [20], based on the conversion factor established by Freireich [21]. Control animals received the same volume of vehicle (PBS). Following injection, rats were housed in metabolic chambers for 72 h for indirect open circuit calorimetry measurements. Rats were monitored and weighed daily. PmFBs were prepared from the red gastrocnemius muscle at three different time points post-injection: 2 h (n= 8 for CTRL; n=8 for DOX), 24 h (n=10 for CTRL; n=6 for DOX), and 72 h (n=15 for CTRL; n=13 for DOX).

Rodent care and reagents

All rodents were housed in the Department of Comparative Medicine at East Carolina University in a temperature- and light-controlled room and given free access to food and water. All procedures were approved by the Institutional Animal Care and Use Committee. Skeletal muscle was obtained from anesthetized rats (100 mg/kg intraperitoneal ketamine-xylazine). Following surgery, rats were euthanized by cervical dislocation under anesthesia. Doxorubicin was purchased from Bedford Laboratories (Bedford, OH). All other chemicals were purchased from Sigma-Aldrich (St. Louis, MO). The Total OxPhos Complex Kit used to measure mitochondrial content was purchased from Invitrogen (Frederick, MD). Fluorescence-conjugated secondary antibodies were purchased from LI-COR (Lincoln, NE).

Determination of body composition

Pre- and post-injection (72 h) measurements of fat and lean body mass were determined using the EchoMRI-500 (Houston, TX) in accordance with the manufacturer's instructions.

Indirect in vivo metabolic parameters

The TSE LabMaster System (TSE Systems, Chesterfield, MO) was used to determine rates of oxygen consumption (VO_2) and carbon dioxide production (VCO_2), respiratory exchange ratio, food and water intake, and energy expenditure. Energy expenditure was calculated by the system using the equation ((CVO_2 * VO_2) + ($CVCO_2$ * VCO_2)/1000). Constants of the equation include: CVO_2 = 3.941 [ml/h] and $CVCO_2$ = 1.106 [ml/h]. All rates are expressed per g of body weight determined every 24 h. Infrared sensors were used to record ambulatory activity in three-dimensional axes (X, Y, Z). Counts across all three axes were summed to give total ambulatory activity.

Permeabilized fiber bundle preparation

Procedures were performed as described previously [22-24]. In brief, fiber bundles from the red portion of the gastrocnemius muscle were separated with fine forceps in ice-cold Buffer X (in mM: 50 K-MES, 35 KCl, 7.23 K_2EGTA, 2.77 CaK_2EGTA, 20 imidazole, 20 taurine, 5.7 ATP, 14.3 PCr, 6.56 $MgCl_2$-$6H_2O$; pH 7.1). After separation, fiber bundles were permeabilized in Buffer X with 40 μg/ml saponin for 30 min and then washed in ice-cold Buffer Z (in mM: 105 K-MES, 30 KCl, 1 EGTA, 10 K_2HPO_4, 5 $MgCl_2$-$6H_2O$, 0.5 mg/ml BSA; pH 7.1) until analysis. A subset of fibers were exposed (15 min) to dithiothreitol (DTT, 1 mM in Buffer Z) following permeabilization before mitochondrial function analysis.

Mitochondrial respiration

High-resolution O_2 consumption measurements were conducted using the OROBOROS Oxygraph-2k (Oroboros Instruments, Innsbruck, Austria) at 37°C with an initial chamber concentration of 300-350 μM oxygen. This concentration does not alter respiratory kinetics [22] and maximizes the duration of experiments before oxygen becomes rate limiting. All experiments were run in Buffer Z containing 20 mM creatine monohydrate and 25 μM blebbistatin (myosin II ATPase inhibitor). Individual protocols included: (1) 2 mM malate + 4 mM ADP followed by sequential additions of glutamate up to 16 mM; (2) 15 mM glutamate + 2 mM malate followed by sequential additions of ADP up to 4 mM; (3) 2 mM malate + 4 mM ADP followed by sequential additions of pyruvate up to 4 mM; (4) 5 mM pyruvate + 2 mM malate followed by sequential additions of ADP up to 4 mM; (5) 10 μM rotenone + 4 mM ADP followed by sequential additions of succinate up to 14 mM; (6) 2 mM malate + 4 mM ADP followed by sequential additions of palmitoylcarnitine up to 75 μM. The Km was determined through the Michaelis-Menten enzyme kinetics using Prism Graphpad (La Jolla, CA). At the end of each protocol cytochrome c was added to test for

mitochondrial membrane integrity. Any PmFB that generated a >10 % increase in respiration following the addition of cytochrome c was not included in the data analysis. At the conclusion of each experiment, PmFBs were washed in dH_2O and dried via freeze-drying (Labconco, Kansas City, MO). Polarographic oxygen measurements are expressed as pmol• s^{-1} • mg^{-1} dry weight.

Mitochondrial H_2O_2 emission

H_2O_2 emission was measured at 37°C in Buffer Z containing 5000 U/mL CuZn-SOD, 25 μM blebbistatin, 50 μM Amplex UltraRed (AUR), and 6 U/mL horseradish peroxidase. Resorufin fluorescence (peroxidation product of AUR) was monitored by the Fluorolog-3 spectrofluorometer (Horiba Jobin Yvon, Edison, NJ) at excitation/emission 568/581 nm. Individual protocols included: (1) 9 mM succinate; (2) 10 mM pyruvate + 2 mM malate + 10 mM glutamate; (3) 25 μM palmitoyl-L-carnitine + 10 mM glycerol-3-phosphate + 10 mM Antimycin A. For each protocol a background fluorescence rate was established in the presence of the PmFB, followed by the addition of subsequent substrates. After correcting for the rate of change in background fluorescence, the concentration of H_2O_2(pmol) was calculated from previously established resorufin fluorescence intensity standard curves with known concentrations of H_2O_2 for each individual protocol. Following each experiment, PmFBs were dried and weighed (as described above) and mitochondrial H_2O_2 emission expressed as pmol• min^{-1} • mg^{-1} dry weight.

Mitochondrial calcium retention capacity

To determine susceptibility to opening of the permeability transition pore (PTP), PmFBs were exposed to progressive calcium loading (20-60 μM) in the presence of (in mM): 5 malate, 10 glycerol-3-phosphate, 10 glutamate, 10 succinate, 15 pyruvate, 0.025 ADP, and 0.002 thapsigargin, to inhibit calcium uptake via the sarco/endoplasmic reticulum Ca-ATPase (SERCA). Changes in extramitochondrial calcium concentration were monitored fluorometrically using Calcium Green (1 μM, excitation/emission 506/532 nm, Invitrogen). All experiments were run at 37°C in Buffer Z containing 2 U/mL hexokinase and 5 mM 2-deoxyglucose (to clamp respiration), and 25 μM blebbistatin. At the conclusion of each experiment, PmFBs were dried and weighed (as described above) and total calcium uptake expressed as pmol • mg^{-1} dry weight.

Mitochondrial Membrane Potential (Δψ)

Δψ and respiration rates of PmFBs were measured simultaneously using the OROBOROS Oxygraph-2k (Oroboros Instruments) combined with electrodes sensitive to TPP^+ (tetraphenylphosponium, a membrane-potential dependent probe) and oxygen at 25°C, as developed by Lin, et al [25]. All experiments were run in Buffer Z containing 20 mM creatine monohydrate and 25 μM blebbistatin. The protocol included: (in mM) 2 malate, 10 glutamate, 15 pyruvate, 10 succinate, 10 glycerol-3-phosphate, 5 2-deoxyglucose, 2 U/mL hexokinase + ADP titration (25, 50, 100, 250, 500, 1000, 2000 μM) + 2 μM FCCP. During the protocol the TPP^+ electrode was calibrated by a 5 point titration (1.1-1.5 μM TPP^+) for quantifying the concentration of TPP^+.

The calculation of Δψ is based on the Nernst equation with binding correction factors and estimated mitochondrial protein content to PmFB freeze-dried weight. The Oroboros TPP^+-Δψ calculation template (www.oroboros.at) was used with the following equation:

$$\Delta\Psi = \frac{RT}{zF} \cdot \ln\left(\frac{\frac{n_{\mathrm{add}}}{c_{\mathrm{ext,free}}} - V_{\mathrm{ext}} - K'_{\mathrm{O}} \cdot P_{\mathrm{C}}}{V_{\mathrm{mt}}\,(\mathrm{spec}) \cdot P_{\mathrm{mt}} + K'_{\mathrm{i}} \cdot P_{\mathrm{mt}}}\right)$$

Variables and constants of the equation include: n_{add} = total amount of ions added to system; $c_{ext,free}$ = free concentration of probe ion outside mitochondria; V_{ext} = volume of external solution outside mitochondria; V_{mt} = volume of mitochondrial matrix (1 μl/mg [26]); K_i' = internal partition coefficient of TPP^+ (7.9 μl/mg [26]); K_o' = external partition coefficient of TPP^+ (14.3 μl/mg [26]); P_{mt} = total mitochondria protein content (7.5% of mg dry weight) [27, 28]; P_c = total cellular protein content (equivalent to PmFB mg dry weight).

Western blot analysis

PmFBs were homogenized in lysis buffer (120 mM Tris, 200 mM DTT, 20% glycerol, 6% SDS, and 0.002% bromophenol blue, pH 7.2) and western blot procedures performed as described previously [7, 8]. Results were normalized for total protein using MemCode Reversible Protein Stain (Pierce, Rockford, IL).

Statistics

Data are presented as mean ± SEM. Statistical analyses were performed using commercial software (Prism GraphPad, La Jolla, CA). Types of tests included Student's t-test for the comparison of two means or ANOVA for comparisons of multiple means. When an overall difference was detected by an ANOVA, a post hoc Bonferroni's test was performed. Statistical significance was accepted when $p<0.05$. Time point experimental groups were compared to their respective time-matched controls. No significant differences existed between control groups from various time point experimental groups; thus for clarity graphs including time-course data display a combined control group for all three time points (2, 24, and 72 h).

RESULTS

Whole-body effects of doxorubicin

In agreement with our previous work [6, 7] and other reports [29], a single doxorubicin injection caused a significant decline in body weight 48-72 h following exposure (% change from CTRL, 24 h: −5 ± 5; 48 hrs: −9 ± 5, $p<0.01$; 72 h: −15 ± 6, $p<0.01$). Whole-body fat (21.3 ± 0.8 g CTRL; 18.9 ± 0.9 g DOX, $p<0.05$) and lean mass (250 ± 5 g CTRL; 207 ± 5 g DOX, $p<0.01$) were reduced 72 h following doxorubicin exposure.

Figure 1 illustrates whole-body metabolism and ambulatory activity measured by indirect calorimetry. Just 24 h following exposure, doxorubicin-treated rats exhibited a 14% decrease in whole-body oxygen consumption that remained depressed during the dark phases of the 72 h experimental period (Fig 1A). Corresponding with the decline in oxygen consumption, ambulatory activity was decreased during the dark phase for the entire 72 h experimental period (Fig 1C). Consistent with a decrease in activity, total energy expenditure was decreased 48-72 h following doxorubicin administration. Respiratory exchange ratios (RER) were lower in doxorubicin-treated rats, implying a greater reliance on lipid metabolism (24 h: 0.82 ± 0.01 CTRL, 0.78 ± 0.01 DOX; 48 h: 0.82 ± 0.01 CTRL, 0.74 ± 0.02 DOX, $p<0.01$; 72 h: 0.82 ± 0.02 CTRL, 0.71 ± 0.02 DOX, $p<0.01$).

Skeletal muscle mitochondrial respiration following doxorubicin administration

To investigate both a short- and long-term effect of doxorubicin on skeletal muscle mitochondrial function, PmFBs were isolated from the red gastrocnemius muscle at three different time points post-injection. Individual protocols tested the kinetics of various complexes in the ETS.

NADH-supported respiration—Maximal state 3 respiration supported with glutamate/malate was depressed just 2 h following doxorubicin exposure, an effect that was reversed at the 24 h time point (Fig 2A). ADP-supported respiration in the presence of maximal glutamate/malate was not altered 2-24 h following administration (Fig 2B). Both state 3 respiration supported with glutamate/malate and the opposite condition, ADP-supported respiration with maximal glutamate/malate, were depressed at all substrate concentrations 72 h following a single doxorubicin injection (Fig 2A & B). Doxorubicin also depressed pyruvate-supported respiration at the 72 h time point. Maximal state 3 respiration supported with pyruvate/malate was depressed following doxorubicin administration (CTRL: 1021 ± 80 pmol• s^{-1} • mg^{-1} dry weight, DOX: 804 ± 67 pmol• s^{-1} • mg^{-1} dry weight, $p<0.05$). In addition, ADP-stimulated respiration supported with pyruvate/malate was significantly reduced (CTRL: 766 ± 49 pmol• s^{-1} • mg^{-1} dry weight, DOX: 478 ± 100 pmol• s^{-1} • mg^{-1} dry weight, $p<0.05$).

$FADH_2$-supported respiration—A similar trend was evident for Complex II-supported respiration; 2 h following doxorubicin exposure, maximal state 3 respiration supported with succinate was reduced (Fig 2C), but then returned to control levels at the 24 h time point. However, 72 h post-injection succinate-supported respiration was depressed compared to controls (Fig 2C).

Doxorubicin is known to depress fatty acid oxidation in cardiac muscle [30], affecting both Complex I- and Complex II-supported respiration. 72 h post-injection doxorubicin depressed maximal state 3 palmitoylcarnitine-supported respiration in skeletal muscle (CTRL: 233 ± 20 pmol• s^{-1} • mg^{-1} dry weight, DOX: 165 ± 16 pmol• s^{-1} • mg^{-1} dry weight, $p<0.05$). There was no change in Km values for any of the substrates evaluated (data not shown).

Doxorubicin-induced mitochondrial H_2O_2 emitting potential

Doxorubicin is known to increase oxidant activity in skeletal muscle [7], along with downstream protein markers of oxidation [7, 16]. However, the source of ROS is unknown. We evaluated the mitochondria as a potential source, measuring H_2O_2 emitting potential in PmFBs following a single doxorubicin injection.

Doxorubicin increased the rate of mitochondrial H_2O_2 emitting potential 2 h post injection by ~52% (Fig 3A). After 24 h, mitochondrial H_2O_2 emission decreased but was still elevated over controls, then continued to decline after 72 h below control levels. The effect of doxorubicin on mitochondrial H_2O_2 emission was determined during respiration supported with the substrate succinate, which elicits reverse electron flow-mediated superoxide production at complex I [31].

To determine if the changes in mitochondrial function induced by doxorubicin may be related to a general oxidation of the mitochondrial matrix, a subset of fibers from the 2 h experimental group were pre-treated with DTT, a strong reducing agent, during the final 15 min of the wash step. Interestingly, mitochondrial H_2O_2 emitting potential increased in the control fibers following DTT exposure, highlighting the numerous mitochondrial proteins that contain reactive thiols and are sensitive to the redox state [32]. Despite the basal increase in control fibers, exposure to DTT did reduce the doxorubicin-induced increase in mitochondrial H_2O_2 emission during respiration supported by succinate (Fig 3B). However, DTT treatment did not restore state 3 glutamate/malate-supported respiration (Fig 3C). Thus, these findings suggest doxorubicin-induced changes in H_2O_2 emitting potential, but not respiratory function, may be mediated by oxidative changes in the mitochondrial matrix, although clearly more targeted experiments are needed to determine the specific components of the redox system involved.

Rates of mitochondrial H_2O_2 emitting potential supported with maximal pyruvate, malate, and glutamate were not different at any time point following doxorubicin exposure (data not shown). Consistent with data obtained during succinate supported respiration, 72 h post-injection palmitoylcarnitine + glycerol-3-phosphate-supported H_2O_2 emission, which also feeds electrons into the ETS beyond complex I, was increased (CTRL: 2.93 ± 0.56 pmol• min^{-1} • mg^{-1} dry weight, DOX: 5.77 ± 1.29 pmol• min^{-1} • mg^{-1} dry weight, p=0.05).

Mitochondrial calcium retention following doxorubicin exposure

The mitochondrial permeability transition pore (mPTP) is sensitive to ROS and regulated by electron flux through complex I in skeletal muscle [33, 34]. Previous reports in cardiac muscle show doxorubicin impairs calcium uptake into the mitochondria and increases susceptibility of the mPTP to calcium-induced opening [35, 36]. Fig 4A illustrates a representative trace of calcium uptake in a PmFB of a control and doxorubicin treated rat at the 72 h time point. The mPTP opened relatively quickly compared to control, requiring only two calcium pulses, indicative of reduced calcium retention capacity and/or increased sensitivity of the mPTP to calcium as a consequence of doxorubicin treatment. Total calcium uptake under state 3 conditions was not impaired at any of the earlier time points following doxorubicin exposure (Fig 4B).

Doxorubicin alters mitochondrial membrane potential

The electron carriers of the mitochondrial ETS drive the translocation of protons across the inner membrane, creating a proton motive force composed of both a chemical and electrical gradient [37]. The electrical potential ($\Delta\psi$) is the dominant component of the proton motive force that drives the synthesis of ATP, and any alterations can provide insight into overall mitochondrial function. As depicted in the control trace (Fig 5, open circles), $\Delta\psi$ decreases (i.e., becomes positive) as ADP is added, indicative of a progressive reduction in proton build up across the inner membrane, higher electron flow through the ETS, and increased oxygen consumption. Just 2 h following doxorubicin exposure, a slight rightward shift in the $JO_2/\Delta\psi$ curve was observed and became more pronounced at 24 h, indicative of a greater reductive pressure within the ETS. This situation increases the potential for electron leak, particularly under basal respiratory conditions, and thereby increases the potential for ROS production. At the 72 h time point, the $JO_2/\Delta\psi$ curve is shifted markedly to the left (Fig 5, closed circles), potentially reflecting an adaptive increase in proton conductance and/or a compromise in respiratory function.

Mitochondrial content in skeletal muscle following doxorubicin exposure

Maximal respiratory capacity (FCCP-stimulated) was determined in the presence of maximal glutamate, pyruvate, malate, glycerol-3-phosphate, succinate, and ADP at the end of the $JO_2/\Delta\psi$ protocol. There was no difference in maximal respiratory capacity between control and doxorubicin treated PmFBs (Fig 6A). In addition, no changes in protein content were detected for any of the complexes (I-V) 72 h following doxorubicin administration (Fig 6B), suggesting mitochondrial content was not altered by doxorubicin treatment.

DISCUSSION

Our novel findings demonstrate that the anticancer agent doxorubicin causes skeletal muscle mitochondrial dysfunction in a time-course dependent manner. Initially, doxorubicin induces a demonstrable inhibition in mitochondrial respiration and a marked increase in H_2O_2 emission, both of which surprisingly are at least partially restored to control levels within 24 h after doxorubicin exposure. However, the relationship between oxygen consumption and $\Delta\psi$ is clearly shifted to the right at 24 h, indicative of elevated reducing pressure within the ETS. By 72 h, this relationship is now shifted to the left, overall respiratory capacity is

compromised, and susceptibility to loss of function is evident (i.e., increased sensitivity to mPTP opening and collapse of proton motive force). These findings at the molecular level provide potential insight into the mechanisms by which doxorubicin causes debilitating muscle weakness and fatigue in cancer patients undergoing chemotherapy.

The biphasic response of skeletal muscle following a single doxorubicin injection is interesting. Initially (2 h) mitochondrial respiratory capacity is decreased in response to both NADH- and $FADH_2$-supported respiration. Very few studies have evaluated the short-term effects of systemic doxorubicin administration on muscle, focusing more on the direct effects following exposure *in vitro*. Despite the difference in methods of exposure, the results correspond. Permeabilized fibers isolated from rat hearts perfused with doxorubicin for 1 hour show a significant decline in state 3 complex I-supported mitochondrial respiration [38]. Parallel findings have also been reported in isolated cardiac mitochondria [11].

Mitochondrial H_2O_2 emission is markedly increased 2 h after doxorubicin administration and remains elevated at 24 h, despite the restored respiratory capacity. Kavazis et al [39] reported no change in respiration (complex I- or II-supported) of cardiac mitochondria 24 h following a single doxorubicin injection. Further experiments from the same study showed a marked increase in mitochondrial H_2O_2 emitting potential during succinate-supported respiration. Additional evidence for increased reducing pressure within the ETS is provided by the $JO_2/\Delta\psi$ curve, with a prominent rightward shift at 24 h. Despite a rescue in the respiratory capacity at 24 h, persistent reducing pressure and elevated H_2O_2 emission can disrupt the normal redox balance within the cell, leading to oxidative damage. Indeed, prolonged doxorubicin exposure depletes vital redox buffering systems, such as glutathione, in striated muscle [40, 41], significantly compromising the ability of the antioxidant buffering system to maintain a proper cellular redox environment.

By 72 h after doxorubicin treatment, respiratory capacity is clearly reduced in skeletal muscle. Isolated mitochondria from cardiac muscle following doxorubicin administration show similar declines in respiratory capacity at later time points. Activity of Complex I and II are dramatically decreased, as well as respiration, both 3 days [13] and 5 days [35] after a single doxorubicin injection. A unique characteristic of this later phase is increased sensitivity to mPTP opening, which results in uncoupling of the respiratory chain and membrane potential collapse [38, 42]. In isolated cardiac mitochondria, doxorubicin promotes the opening of the mPTP 4-7 days after an injection [43, 44]. In skeletal muscle, total calcium uptake was impaired 72 h following doxorubicin exposure, resulting in a rapid opening of the mPTP.

Two potential sources of doxorubicin-induced oxidants are: (1) redox cycling of doxorubicin with Complex I of the mitochondria, and (2) inactivation of the ETS. A quinone moiety in doxorubicin's structure can be transformed into a semiquinone via one-electron reduction by complex I [45]. The semiquinone then reacts with molecular oxygen to produce a superoxide anion. Doxorubicin then returns to the quinone form, with the cycle continuing as long as NADH is present [46]. Elevated H_2O_2 from this cycling can lead to a variety of redox modifications of numerous macromolecules. In the presence of redox active iron (e.g. Fe (II), Fe-O complexes), H_2O_2 forms hydroxyl radicals leading to lipid peroxidation [17, 47]. Mitochondrial and myofilament proteins are altered with elevated oxidants, extensively effecting metabolism and contractile function [14, 15].

To determine whether the increase in H_2O_2 emitting potential in skeletal muscle may be mediated by an oxidative shift in redox environment, we exposed a subset of PmFBs to DTT, a strong reducing agent, *in vitro*. The increase in mitochondrial H_2O_2 emitting

potential evident within 2 h following doxorubicin administration was reduced by DTT. This suggests the mechanism(s) contributing to the elevated H_2O_2 emitting potential with doxorubicin are likely due to redox modifications within the matrix (e.g., the ETS, redox buffering system, etc.). H_2O_2 emission was assessed in the current study during state 4 respiration supported by succinate, which induces reverse electron flow and superoxide generation at the ubiquinone binding site of complex I [31]. This suggests Complex I may be subject to redox modifications that alter its susceptibility to leaking electrons and generating superoxide. Indeed, numerous pathologies are associated with genetic deficiencies in Complex I, nearly all of which are redox modulated [48]. Further, more targeted studies are required to determine the specific components of the redox system that may be modified by doxorubicin.

The second potential source of oxidants caused by doxorubicin is direct inhibition of the complexes of the ETS. In isolated heart mitochondria, doxorubicin inhibits the enzyme's oxidase (or electron transferring) property by physically inhibiting the active site [46]. Non-functional ETS complexes lead to the diversion of electrons to form increased amounts of free-radical superoxide, and ultimately H_2O_2. Two potential sources of doxorubicin-induced oxidants doubles the risk for a compromised cellular redox environment, increasing the susceptibility of damage at the whole organ level.

Whole-body metabolism was significantly affected by doxorubicin exposure. Energy expenditure was decreased 48-72 h following doxorubicin administration, suggesting a decrease in overall basal oxidative metabolism. The same decrease in energy expenditure was seen in cancer patients receiving a doxorubicin-based chemotherapy regimen. Patients displayed a steady decline in resting energy expenditure over five days while receiving chemotherapy, with no change in nutritional status or physical activity [49]. In addition to a disturbance in energy balance due to inhibition of the ETS, energy stores could also be affected. Mitochondrial creatine kinase activity, an important enzyme for balance of energy metabolites and regulation of oxidative phosphorylation, is decreased in cardiac muscle 72 h following doxorubicin administration [13]. These findings suggest an inability of the organism to maintain energy homeostasis, which is likely a two-part problem: cardiac insufficiency and skeletal muscle dysfunction.

A deficit in the ability to meet energy demand becomes apparent at the whole-body level when a person becomes fatigued, a universal symptom in cancer chemotherapy. Cancer patients that have undergone chemotherapy display physiological fatigue as evidenced by decreased gait speed, slower chair rise time, and reduced maximal grip strength along with an accelerated rate of hand-grip fatigue [3, 50-53]. These measurements take into account both cardiac and skeletal muscle systems that contribute to the overall energy status of the cell. While the two organ systems cannot be separated for whole-body measurements, studies that specifically assess muscle strength suggest skeletal muscle is an important factor in the documented clinical fatigue.

Our previous work [6-8], along with others [29, 54, 55], demonstrates skeletal muscle from healthy rodents exposed to doxorubicin show a decrease in muscle strength and an accelerated rate of fatigue. Muscle weakness can result from impaired membrane excitability, calcium release/uptake, and/or myofibrillar protein function. All of these possible endpoints can be dramatically affected by both the energy status and the redox environment of the myocyte [56, 57]. The combined effect of disrupted metabolism and redox signaling caused by doxorubicin can negatively affect fundamental muscle function, and contribute to the disabling whole-body symptoms observed in cancer patients.

This dilemma of debilitating muscle weakness and fatigue in cancer patients is not unsolvable. A similar problem existed in the clinic over twenty years ago. At the time, nausea and vomiting were inevitable adverse events that cancer patients had to manage. In the early 1990s antiemetic agents were introduced and are now a standard clinical practice to help patients abolish the distressing side effects, often times leading to improved retention rates and enhanced quality of life during treatment [58]. It is anticipated that deciphering the underlying mechanism of chemotherapy-induced muscle weakness and fatigue will provide the basis for the development of targeted countermeasure strategies.

Acknowledgments

This project was supported by National Institutes of Diabetes and Digestive and Kidney Diseases (R01-DK073488, PDN) and Arthritis and Musculoskeletal and Skin Diseases (F32-AR061946, LAG) of the National Institutes of Health. The content is solely the responsibility of the authors and does not necessarily represent the official views of the National Institutes of Health.

REFERENCES

[1]. Chabner, BA.; Ryan, DP.; Paz-Ares, L.; Garcia-Carbonero, R.; Calabresi, P.; Hardman, JG.; Limbird, LE.; Gilman, AG. Goodman & Gilman's The pharmacologic basis of therapeutics. McGraw-Hill, Medical Publishing Division; New York: 2001.

[2]. Swain SM, Whaley FS, Ewer MS. Congestive heart failure in patients treated with doxorubicin: a retrospective analysis of three trials. Cancer. 2003; 97:2869–2879. [PubMed: 12767102]

[3]. Schwartz AL. Daily fatigue patterns and effect of exercise in women with breast cancer. Cancer Pract. 2000; 8:16–24. [PubMed: 10732535]

[4]. Jacobsen PB, Hann DM, Azzarello LM, Horton J, Balducci L, Lyman GH. Fatigue in women receiving adjuvant chemotherapy for breast cancer: characteristics, course, and correlates. J Pain Symptom Manage. 1999; 18:233–242. [PubMed: 10534963]

[5]. Gilliam LA, St Clair DK. Chemotherapy-induced weakness and fatigue in skeletal muscle: The role of oxidative stress. Antioxid Redox Signal. 2011

[6]. Gilliam LA, Ferreira LF, Bruton JD, Moylan JS, Westerblad H, St Clair DK, Reid MB. Doxorubicin acts through tumor necrosis factor receptor subtype 1 to cause dysfunction of murine skeletal muscle. J Appl Physiol. 2009; 107:1935–1942. [PubMed: 19779154]

[7]. Gilliam LA, Moylan JS, Ann Callahan L, Sumandea MP, Reid MB. Doxorubicin causes diaphragm weakness in murine models of cancer chemotherapy. Muscle Nerve. 2011; 43:94–102. [PubMed: 21171100]

[8]. Gilliam LA, Moylan JS, Ferreira LF, Reid MB. TNF/TNFR1 signaling mediates doxorubicin-induced diaphragm weakness. Am J Physiol Lung Cell Mol Physiol. 2011; 300:L225–231. [PubMed: 21097524]

[9]. Bower JE, Ganz PA, Desmond KA, Bernaards C, Rowland JH, Meyerowitz BE, Belin TR. Fatigue in long-term breast carcinoma survivors: a longitudinal investigation. Cancer. 2006; 106:751–758. [PubMed: 16400678]

[10]. Sarvazyan N. Visualization of doxorubicin-induced oxidative stress in isolated cardiac myocytes. Am J Physiol. 1996; 271:H2079–2085. [PubMed: 8945928]

[11]. Davies KJ, Doroshow JH. Redox cycling of anthracyclines by cardiac mitochondria. I. Anthracycline radical formation by NADH dehydrogenase. J Biol Chem. 1986; 261:3060–3067. [PubMed: 3456345]

[12]. Xiong Y, Liu X, Lee CP, Chua BH, Ho YS. Attenuation of doxorubicin-induced contractile and mitochondrial dysfunction in mouse heart by cellular glutathione peroxidase. Free Radic Biol Med. 2006; 41:46–55. [PubMed: 16781452]

[13]. Yen HC, Oberley TD, Gairola CG, Szweda LI, St Clair DK. Manganese superoxide dismutase protects mitochondrial complex I against adriamycin-induced cardiomyopathy in transgenic mice. Arch Biochem Biophys. 1999; 362:59–66. [PubMed: 9917329]

[14]. Supinski GS, Callahan LA. Free radical-mediated skeletal muscle dysfunction in inflammatory conditions. J Appl Physiol. 2007; 102:2056–2063. [PubMed: 17218425]

[15]. Shigenaga MK, Hagen TM, Ames BN. Oxidative damage and mitochondrial decay in aging. Proc Natl Acad Sci U S A. 1994; 91:10771–10778. [PubMed: 7971961]

[16]. Smuder AJ, Kavazis AN, Min K, Powers SK. Exercise protects against doxorubicin-induced oxidative stress and proteolysis in skeletal muscle. J Appl Physiol. 2011; 110:935–942. [PubMed: 21310889]

[17]. Brand MD. The sites and topology of mitochondrial superoxide production. Exp Gerontol. 2010; 45:466–472. [PubMed: 20064600]

[18]. Powers SK, Jackson MJ. Exercise-induced oxidative stress: cellular mechanisms and impact on muscle force production. Physiol Rev. 2008; 88:1243–1276. [PubMed: 18923182]

[19]. Gilliam LA, Moylan JS, Patterson EW, Smith JD, Wilson AS, Rabbani Z, Reid MB. Doxorubicin acts via mitochondrial ROS to stimulate catabolism in C2C12 myotubes. Am J Physiol Cell Physiol. 2012; 302:C195–202. [PubMed: 21940668]

[20]. Glass B, Kloess M, Bentz M, Schlimok G, Berdel WE, Feller A, Trumper L, Loeffler M, Pfreundschuh M, Schmitz N. Dose-escalated CHOP plus etoposide (MegaCHOEP) followed by repeated stem cell transplantation for primary treatment of aggressive high-risk non-Hodgkin lymphoma. Blood. 2006; 107:3058–3064. [PubMed: 16384932]

[21]. Freireich EJ, Gehan EA, Rall DP, Schmidt LH, Skipper HE. Quantitative comparison of toxicity of anticancer agents in mouse, rat, hamster, dog, monkey, and man. Cancer Chemother Rep. 1966; 50:219–244. [PubMed: 4957125]

[22]. Perry CG, Kane DA, Lin CT, Kozy R, Cathey BL, Lark DS, Kane CL, Brophy PM, Gavin TP, Anderson EJ, Neufer PD. Inhibiting myosin-ATPase reveals a dynamic range of mitochondrial respiratory control in skeletal muscle. Biochem J. 2011; 437:215–222. [PubMed: 21554250]

[23]. Kane DA, Anderson EJ, Price JW 3rd, Woodlief TL, Lin CT, Bikman BT, Cortright RN, Neufer PD. Metformin selectively attenuates mitochondrial H2O2 emission without affecting respiratory capacity in skeletal muscle of obese rats. Free Radic Biol Med. 2010; 49:1082–1087. [PubMed: 20600832]

[24]. Anderson EJ, Lustig ME, Boyle KE, Woodlief TL, Kane DA, Lin CT, Price JW 3rd, Kang L, Rabinovitch PS, Szeto HH, Houmard JA, Cortright RN, Wasserman DH, Neufer PD. Mitochondrial H2O2 emission and cellular redox state link excess fat intake to insulin resistance in both rodents and humans. J Clin Invest. 2009; 119:573–581. [PubMed: 19188683]

[25]. Lin CT, Fisher-Wellman KH, Perry CG, Kozy R, Lark DS, Gilliam LA, Smith CD, Neufer PD. Low intensity exercise attenuates acute lipid loading-induced alterations in mitochondrial function in rat skeletal muscle. FASEB J. 2012; 26:1144–1111.

[26]. Labajova A, Vojtiskova A, Krivakova P, Kofranek J, Drahota Z, Houstek J. Evaluation of mitochondrial membrane potential using a computerized device with a tetraphenylphosphonium-selective electrode. Anal Biochem. 2006; 353:37–42. [PubMed: 16643832]

[27]. Jackman MR, Willis WT. Characteristics of mitochondria isolated from type I and type IIb skeletal muscle. Am J Physiol. 1996; 270:C673–678. [PubMed: 8779934]

[28]. Ogata T, Yamasaki Y. Scanning electron-microscopic studies on the three-dimensional structure of mitochondria in the mammalian red, white and intermediate muscle fibers. Cell Tissue Res. 1985; 241:251–256. [PubMed: 4028126]

[29]. Hydock DS, Lien CY, Jensen BT, Schneider CM, Hayward R. Characterization of the effect of in vivo doxorubicin treatment on skeletal muscle function in the rat. Anticancer Res. 2011; 31:2023–2028. [PubMed: 21737618]

[30]. Carvalho RA, Sousa RP, Cadete VJ, Lopaschuk GD, Palmeira CM, Bjork JA, Wallace KB. Metabolic remodeling associated with subchronic doxorubicin cardiomyopathy. Toxicology. 2010; 270:92–98. [PubMed: 20132857]

[31]. Murphy MP. How mitochondria produce reactive oxygen species. Biochem J. 2009; 417:1–13. [PubMed: 19061483]

[32]. Costa NJ, Dahm CC, Hurrell F, Taylor ER, Murphy MP. Interactions of mitochondrial thiols with nitric oxide. Antioxid Redox Signal. 2003; 5:291–305. [PubMed: 12880484]

[33]. Connern CP, Halestrap AP. Recruitment of mitochondrial cyclophilin to the mitochondrial inner membrane under conditions of oxidative stress that enhance the opening of a calcium-sensitive non-specific channel. Biochem J. 1994; 302(Pt 2):321–324. [PubMed: 7522435]

[34]. Fontaine E, Eriksson O, Ichas F, Bernardi P. Regulation of the permeability transition pore in skeletal muscle mitochondria. Modulation By electron flow through the respiratory chain complex i. J Biol Chem. 1998; 273:12662–12668. [PubMed: 9575229]

[35]. Ascensao A, Lumini-Oliveira J, Machado NG, Ferreira RM, Goncalves IO, Moreira AC, Marques F, Sardao VA, Oliveira PJ, Magalhaes J. Acute exercise protects against calcium-induced cardiac mitochondrial permeability transition pore opening in doxorubicin-treated rats. Clin Sci (Lond). 2011; 120:37–49. [PubMed: 20666733]

[36]. Montaigne D, Marechal X, Preau S, Baccouch R, Modine T, Fayad G, Lancel S, Neviere R. Doxorubicin induces mitochondrial permeability transition and contractile dysfunction in the human myocardium. Mitochondrion. 2011; 11:22–26. [PubMed: 20599629]

[37]. Fisher-Wellman KH, Neufer PD. Linking mitochondrial bioenergetics to insulin resistance via redox biology. Trends Endocrinol Metab. 2012; 23:142–153. [PubMed: 22305519]

[38]. Montaigne D, Marechal X, Baccouch R, Modine T, Preau S, Zannis K, Marchetti P, Lancel S, Neviere R. Stabilization of mitochondrial membrane potential prevents doxorubicin-induced cardiotoxicity in isolated rat heart. Toxicol Appl Pharmacol. 2010; 244:300–307. [PubMed: 20096298]

[39]. Kavazis AN, Smuder AJ, Min K, Tumer N, Powers SK. Short-term exercise training protects against doxorubicin-induced cardiac mitochondrial damage independent of HSP72. Am J Physiol Heart Circ Physiol. 2010; 299:H1515–1524. [PubMed: 20833957]

[40]. Li T, Danelisen I, Singal PK. Early changes in myocardial antioxidant enzymes in rats treated with adriamycin. Mol Cell Biochem. 2002; 232:19–26. [PubMed: 12030376]

[41]. Mohamed HE, Asker ME, Ali SI, el-Fattah TM. Protection against doxorubicin cardiomyopathy in rats: role of phosphodiesterase inhibitors type 4. J Pharm Pharmacol. 2004; 56:757–768. [PubMed: 15231041]

[42]. Halestrap AP, Clarke SJ, Javadov SA. Mitochondrial permeability transition pore opening during myocardial reperfusion--a target for cardioprotection. Cardiovasc Res. 2004; 61:372–385. [PubMed: 14962470]

[43]. Solem LE, Henry TR, Wallace KB. Disruption of mitochondrial calcium homeostasis following chronic doxorubicin administration. Toxicol Appl Pharmacol. 1994; 129:214–222. [PubMed: 7527602]

[44]. Marechal X, Montaigne D, Marciniak C, Marchetti P, Hassoun SM, Beauvillain JC, Lancel S, Neviere R. Doxorubicin-induced cardiac dysfunction is attenuated by ciclosporin treatment in mice through improvements in mitochondrial bioenergetics. Clin Sci (Lond). 2011; 121:405–413. [PubMed: 21605084]

[45]. Chen Y, Jungsuwadee P, Vore M, Butterfield DA, St Clair DK. Collateral damage in cancer chemotherapy: oxidative stress in nontargeted tissues. Mol Interv. 2007; 7:147–156. [PubMed: 17609521]

[46]. Marcillat O, Zhang Y, Davies KJ. Oxidative and non-oxidative mechanisms in the inactivation of cardiac mitochondrial electron transport chain components by doxorubicin. Biochem J. 1989; 259:181–189. [PubMed: 2719642]

[47]. Qian SY, Buettner GR. Iron and dioxygen chemistry is an important route to initiation of biological free radical oxidations: an electron paramagnetic resonance spin trapping study. Free Radic Biol Med. 1999; 26:1447–1456. [PubMed: 10401608]

[48]. Raha S, Robinson BH. Mitochondria, oxygen free radicals, disease and ageing. Trends Biochem Sci. 2000; 25:502–508. [PubMed: 11050436]

[49]. Delarue J, Lerebours E, Tilly H, Rimbert A, Hochain P, Guedon C, Piguet H, Colin R. Effect of chemotherapy on resting energy expenditure in patients with non-Hodgkin's lymphoma. Results of a sequential study. Cancer. 1990; 65:2455–2459. [PubMed: 2337860]

[50]. Galvao DA, Taaffe DR, Spry N, Joseph D, Turner D, Newton RU. Reduced muscle strength and functional performance in men with prostate cancer undergoing androgen suppression: a

comprehensive cross-sectional investigation. Prostate Cancer Prostatic Dis. 2009; 12:198–203. [PubMed: 18852703]

[51]. Cantarero-Villanueva I, Fernandez-Lao C, Diaz-Rodriguez L, Fernandez-de-Las-Penas C, Ruiz JR, Arroyo-Morales M. The handgrip strength test as a measure of function in breast cancer survivors: relationship to cancer-related symptoms and physical and physiologic parameters. Am J Phys Med Rehabil. 2012; 91:774–782. [PubMed: 22760108]

[52]. Brown DJ, McMillan DC, Milroy R. The correlation between fatigue, physical function, the systemic inflammatory response, and psychological distress in patients with advanced lung cancer. Cancer. 2005; 103:377–382. [PubMed: 15558809]

[53]. Stone P, Hardy J, Broadley K, Tookman AJ, Kurowska A, A'Hern R. Fatigue in advanced cancer: a prospective controlled cross-sectional study. Br J Cancer. 1999; 79:1479–1486. [PubMed: 10188894]

[54]. Ge M, Fang YY, Liu GP, Guan SD. Effect of Shengmai Injection () on diaphragmatic contractility in doxorubicin-treated rats. Chin J Integr Med. 2012

[55]. Ertunc M, Sara Y, Korkusuz P, Onur R. Differential contractile impairment of fast- and slow-twitch skeletal muscles in a rat model of doxorubicin-induced congestive heart failure. Pharmacology. 2009; 84:240–248. [PubMed: 19776660]

[56]. Allen DG, Lamb GD, Westerblad H. Skeletal muscle fatigue: cellular mechanisms. Physiol Rev. 2008; 88:287–332. [PubMed: 18195089]

[57]. Callahan LA, She ZW, Nosek TM. Superoxide, hydroxyl radical, and hydrogen peroxide effects on single-diaphragm fiber contractile apparatus. J Appl Physiol. 2001; 90:45–54. [PubMed: 11133892]

[58]. Jordan K, Kasper C, Schmoll HJ. Chemotherapy-induced nausea and vomiting: current and new standards in the antiemetic prophylaxis and treatment. Eur J Cancer. 2005; 41:199–205. [PubMed: 15661543]

HIGHLIGHTS

- Skeletal muscle mitochondria demonstrate a biphasic response to a single doxorubicin injection.
- Doxorubicin increases mitochondrial H_2O_2 emission in skeletal muscle
- Elevated reducing pressure in the ETS following doxorubicin administration
- Rats exposed to doxorubicin exhibit decreased whole-body energy expenditure

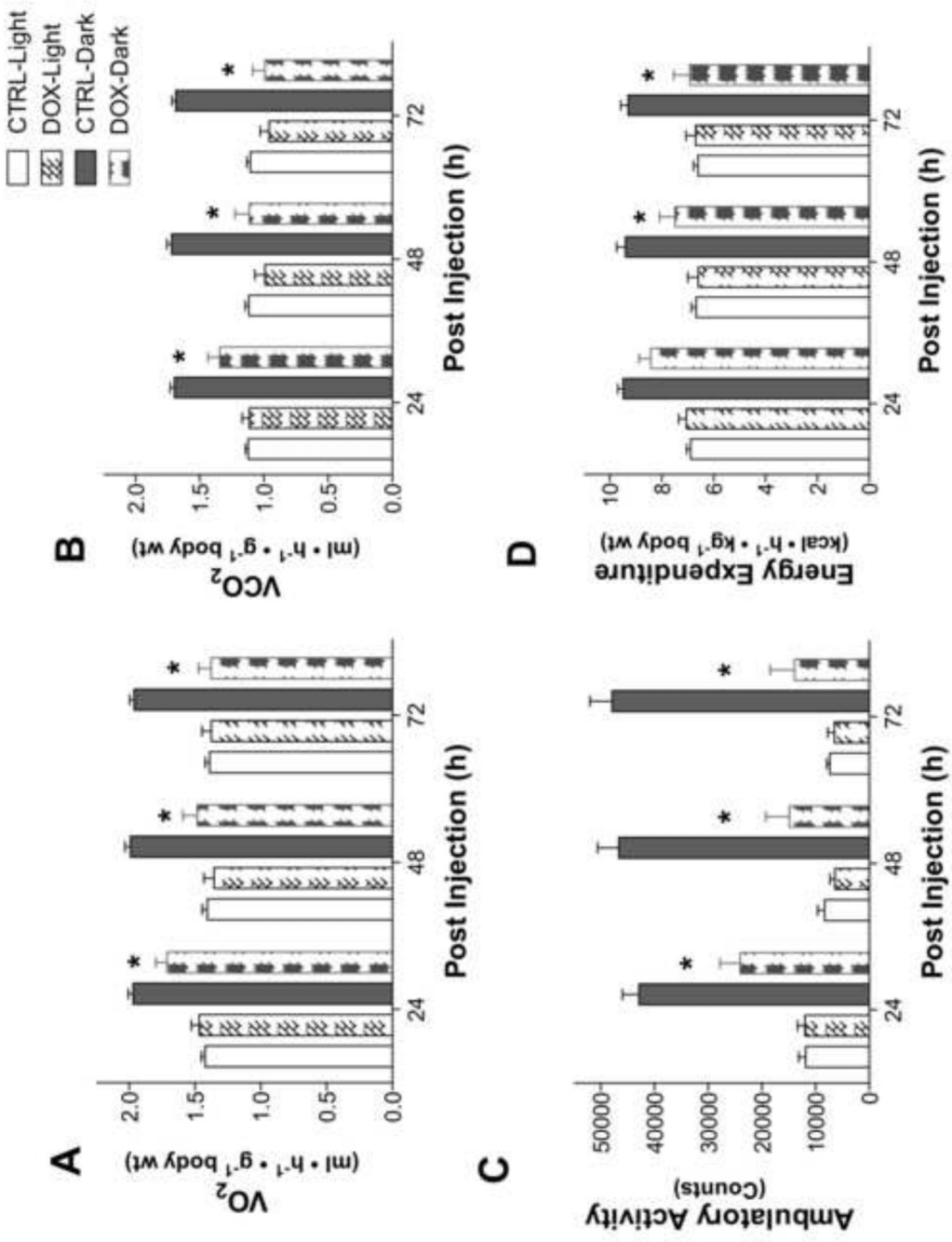

Figure 1. Rats exposed to doxorubicin exhibit decreased whole-body energy expenditure

Indirect metabolic calorimetry and ambulatory activity in rats following doxorubicin administration. (A) Oxygen consumption; (B) carbon dioxide production; (C) ambulatory activity; and (D) calculated energy expenditure. Data are mean ± SEM; $p<0.05$ for overall differences by repeated-measures ANOVA; *$p<0.05$ vs. CTRL in dark phase

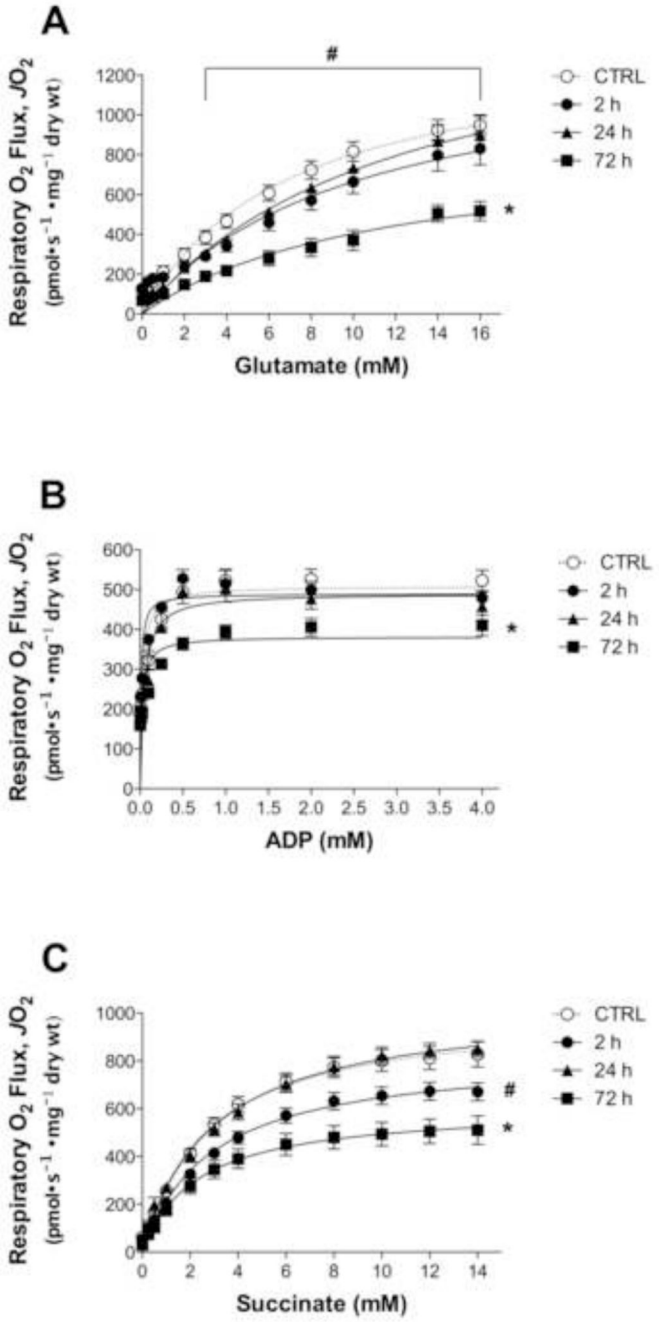

Figure 2. Doxorubicin inhibits NADH- and $FADH_2$-supported respiration in skeletal muscle

Permeabilized myofibers were prepared 2-72 h following doxorubicin administration, and mitochondrial respiratory kinetics were measured. State 3 respiration was measured during (A) glutamate/malate or (C) succinate titration in the presence of maximal ADP (4 mM), and during (B) ADP titration in the presence of maximal glutamate/malate (15/2 mM). Data are mean ± SEM; $p<0.05$ vs. CTRL for 2 h (#) and 72 h (*) for all substrate concentrations unless otherwise denoted by a horizontal line that signifies differences for concentrations 3-16 mM.

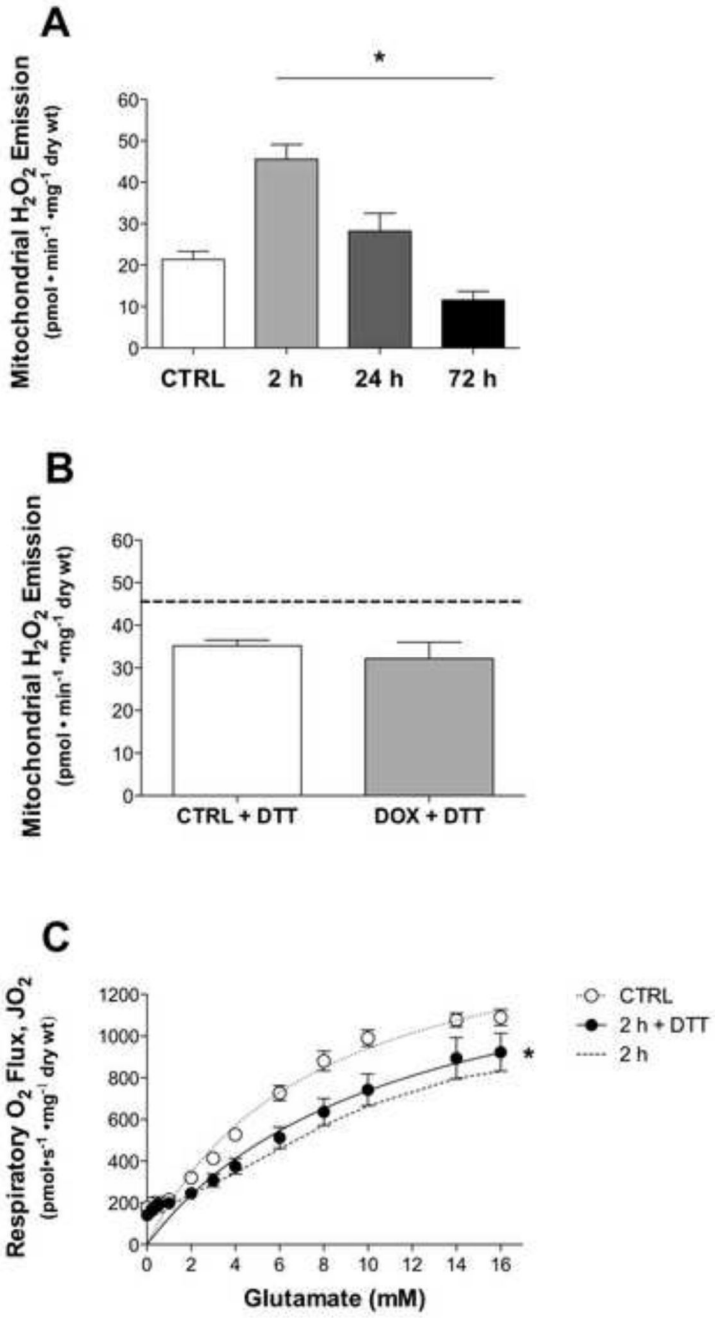

Figure 3. Doxorubicin effects mitochondrial H_2O_2 emission

Mitochondrial H_2O_2 emitting potential of permeabilized myofibers from control (open) and doxorubicin (closed) treated rats (A) 2-72 h and (B) 2 h (+ 1 mM DTT) following injection. Substrate conditions were in the presence of maximal succinate. (C) Maximal state 3 respiration with glutamate/malate of fibers from 2 h experimental group exposed to DTT for 15 min in wash. Dotted line represents previous data from 2 h doxorubicin-treated group (Fig 2A). Data are mean ± SEM; *p<0.05 vs. CTRL.

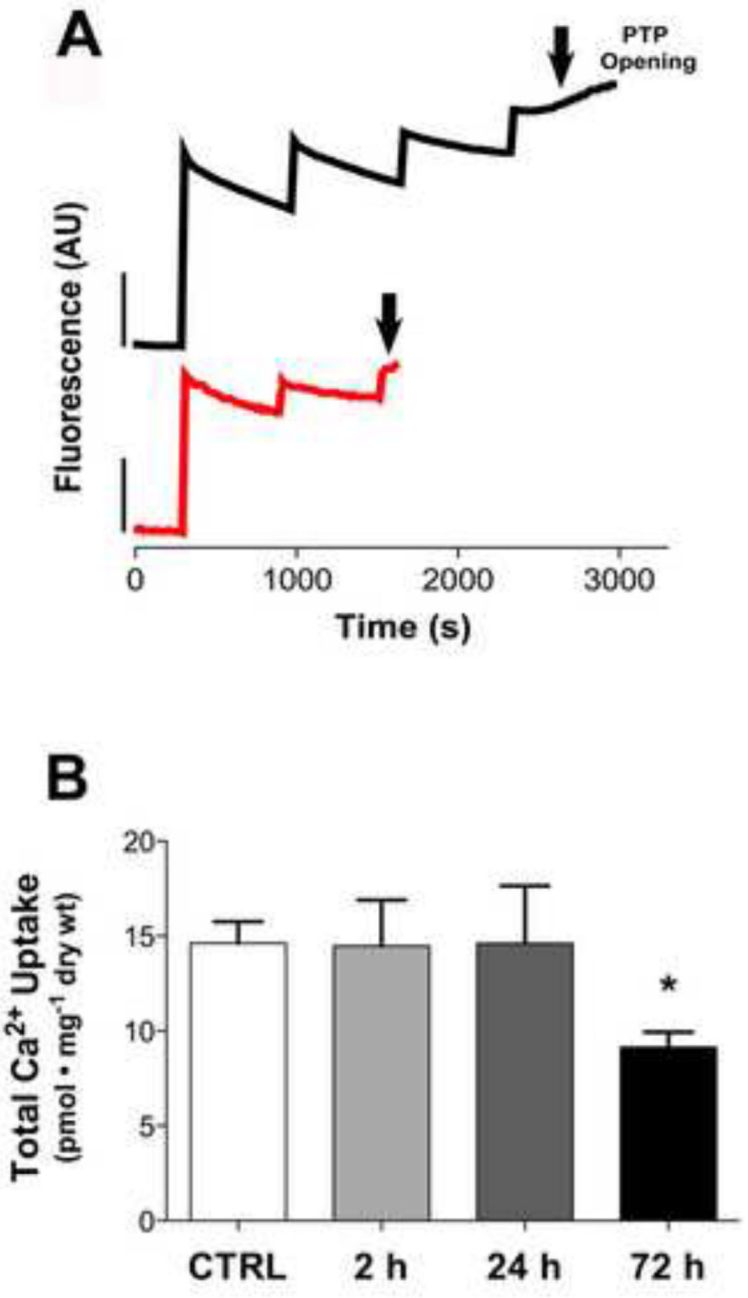

Figure 4. Doxorubicin impairs mitochondrial calcium retention in skeletal muscle

(A) Representative fluorescence trace of calcium uptake in control (black) and doxorubicin (red) myofibers from 72 h experimental group. (B) Total mitochondrial calcium uptake of permeabilized fibers from control (open) and doxorubicin (closed) treated rats 2-72 h following administration. Substrate conditions were in the presence of maximal malate, glycerol-3-phosphate, glutamate, succinate, pyruvate, and 25 μM ADP. Data are mean ± SEM; *p<0.05 vs. CTRL.

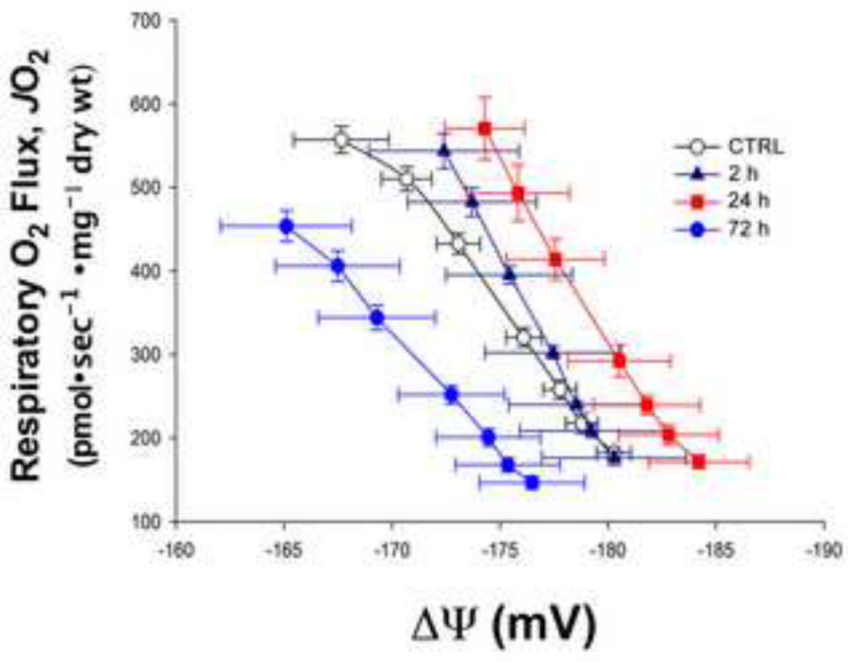

Figure 5. Fluctuations of mitochondrial membrane potential (Δψ) in skeletal muscle following doxorubicin administration

Respiration (JO_2) and membrane potential ($\Delta\psi_m$) monitored simultaneously during ADP-supported respiration in the presence of maximal glutamate, pyruvate, malate, glycerol-3-phosphate, and succinate. Data are mean ± SEM.

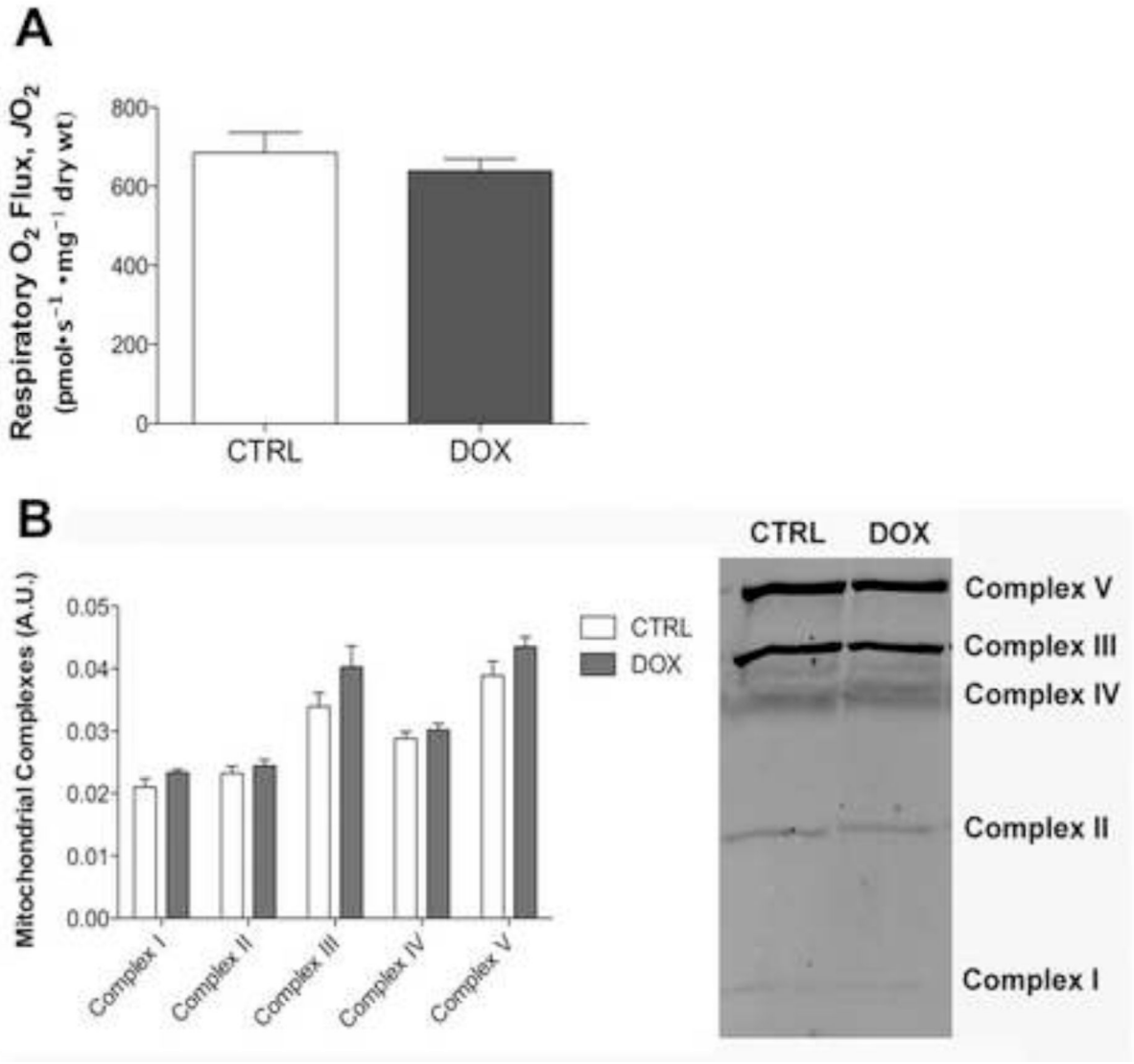

Figure 6. Doxorubicin does not alter mitochondrial content in skeletal muscle

Mitochondrial content evaluated in permeabilized myofibers isolated 72 h following doxorubicin exposure by (A) maximal FCCP-response in the presence of State 3 respiration supported with maximal glutamate, pyruvate, malate, glycerol-3-phosphate, and succinate and by (B) western blot of mitochondrial complexes. Data are mean ± SEM